Master's Thesis of Engineering

# Soft Three-Axis Load Cell using Liquid-Filled 3D Microchannels Embedded in a Highly Deformable Elastomer

3차원 마이크로채널이 내장된 대변형
탄성중합체를 이용한 3축 소프트 로드셀

August 2018

Graduate School of Engineering
Seoul National University
Mechanical Engineering Major

Taekyoung Kim

# 3차원 마이크로채널이 내장된 대변형 탄성중합체를 이용한 3축 소프트 로드셀

## Soft Three-Axis Load Cell using Liquid-Filled 3D Microchannels mbedded in a Highly Deformable Elastomer

Advisor Yong-Lae Park

Submitting a master's thesis of Public Administration

April 2018

Graduate School of Engineering
Seoul National University
Mechanical Engineering Major

Taekyoung Kim

Confirming the master's thesis written by
Taekyoung Kim
June 2018

| | | |
|---|---|---|
| Chair | Suk-Won Cha | (Seal) |
| Vice Chair | Yong-Lae Park | (Seal) |
| Examiner | Yoon Seog Lee | (Seal) |

# Abstract

The advances in soft robotics have increased the need of soft sensors in various applications involved with physical interactions between humans and robots. In this paper, we propose a soft multi-axis force sensor made of multi-material elastomer layers and embedded microfluidic channels that are sensitive to compression perpendicular to the channel's length. The microchannels are geometrically divided into multiple segments for detecting forces in three axes. When a force is applied to the top surface of the sensor, the microchannels are compressed by multi-segmented force plates made of rigid plastic. While the microchannels located on the sides in the structure detect shear forces, the microchannel at the bottom detects normal force. The three-dimensional configuration of the microchannel physically separates the side channels from the bottom channel and consequently enables mechanical decoupling of shear forces from normal force. This paper describes the design and fabrication of the proposed sensor and discusses the experimental results for sensor characterization.

**Keyword** : Soft Robotics, Microfluidic Pressure Sensor, 3D Microchannel, Multi-Axis Force Sensing, Human-Robot Interaction
**Student Number** : 2016-27511

# Table of Contents

# Chapter 1. Introduction

Soft robotics technologies have been implemented to a wide range of robotics applications in recent years, such as medical robots [1], [2], wearable robots [3], [4] and mobile robots [5], [6]. They are particularly useful when the robots are involved with physical interactions with human users. For robots to be more interactive and compatible with humans, they need to be compliant and highly responsive when they are in contact with humans or external objects. To meet this requirement, different types of soft sensors have been developed. Examples include sensors made of elastomer materials mixed with conductive fillers, such as nanowires [7], [8], [9], nanotubes [10], carbon particles [11], [12], and graphene [13], [14], and embedded with liquid conductors, such as liquid metals [15], [16] conductive inks [17], [18], and ionic liquids [19], [20], [21]. Hydrogel soft sensors [22], [23] and optical soft sensors [24], [25] have also been proposed for increased bio-compatibility.

Most of the above sensors rely on sensing mechanisms that detect single-axis deformation, such as a simple one-dimensional normal force or axial strain. However, in many robotics applications, force information with three-dimensional (3D) vector components is highly useful for control. Therefore, efforts have been made to develop soft sensors that can detect forces in 3D, such as multi-axis force sensors using flexible capacitors embedded in polymer

structures [26], [27] and using microfluidic pressure sensitive channels [28], [29]. Although they can detect multi-axis forces, planar (i.e. shear) forces can be detected only when they are combined with a vertical (i.e. normal) force, which not only makes the sensitivity to the shear forces much smaller than that to the normal force but also makes it difficult to decouple the normal force from the shear force. Therefore, we propose a new design of soft sensors (Figure. 1 and Figure. 2) that can detect multi-axis forces not only with increased spatial (or angular) resolution but also with an improved shear force sensitivity through a mechanism that directly detects planar components of the applied force in different angles [30], [31]. Differently from previous sensors that have all the sensing elements located below the pressure point, our design has a 3D microchannel (Figure. 3) that is divided into sidewall and bottom channels, making possible to mechanically decouple shear and normal forces.

In the rest of the paper, we describe the design and fabrication of the proposed soft sensor in Chapters 2 and 3, respectively, presents the experimental setup and the characterization results in Chapter 4, respectively, followed by considerations on materials in Chapter 5 and calibration sensor using a machine learning technique in Chapter 6, and finally conclude and discuss future work in Chapter 7.

# Chapter 2. Design

## 2.1. Sensing Mechanism

  The basic sensing mechanism of the proposed sensor is detection of changes in electrical resistance of the embedded microchannel in a soft structure. The microchannels are filled with eutectic gallium－indium (EGaIn), a liquid－phase metal at room temperature [32]. By embedding multi－segmented force plates on top of the bottom channel and inside of the sidewall channels (Figure. 1－a), different channels will be compressed based on the direction of the force (Figure. 1－b).

## 2.2. Sensor Structure

  The structure of the proposed sensor can be divided into two areas: the internal sensing area and the housing area. The internal sensing area is made of soft elastomer materials (Ecoflex 0030 and Ecoflex 0050, Smooth－On) including embedded EGaIn microchannels connected in series (Figure. 2－a) and six 3D－printed force plates made of rigid plastic. The external housing area is made of a stiffer elastomer (Dragon Skin 30, Smooth On). The stiffer housing plays a role as a backing for the microchannels and facilitates compression of the microchannels when a force is applied.

The moduli of the materials used in our sensor are less than 100 kPa for the sensing area and less than 600 kPa for the housing area. The proposed sensor is flexible enough (Figure. 3-c) to be used as skin for robots for physical interactions with humans.

(a)

35 mm

5 mm

Sensing Structure          Housing

Microchannels   Force plates   Soft polymer   Stiff polymer

(b)

Force

2.5 mm

Sliding

0.4 mm

Microchannel
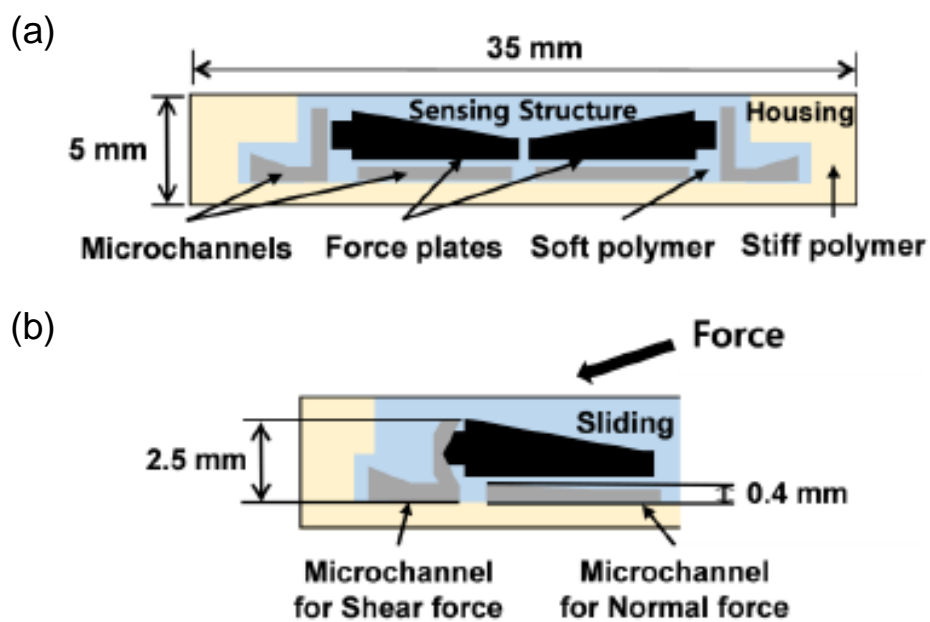for Shear force

Microchannel
for Normal force

**Figure. 1.** Design of a soft multi-axis load cell (a) sensor structure, (b) showing sensing mechanism.

## 2.3. Configuration of Microchannels

The microchannels are located both at the bottom and on the sides of the force plates in the sensing structure (Figure. 1-a). The microchannel (Channel 4 in Figure. 2-a, 250 mm×250 mm, square cross-section) located underneath the force plates detects normal force. Since it covers almost the entire area of the six force plates, a normal force applied anywhere on the force plates can be easily detected. The sidewall microchannels (Channels 1-3 and 5-7 in Figure. 2-a, 250 mm×250 mm and 250 mm×2500 mm) with 3D shapes (Figures. 1-a and 2-a) are divided into six segments and each segment was connected to its own signal wire for detecting a planar force in multi-directions. If a force is applied to the center of the sensor, one or more force plates will be displaced, compressing part of the bottom microchannel and one or two sidewall microchannels corresponding to the direction of the applied force. Therefore, it is possible to decouple the normal and the shear force components.

## 2.4. Force Plates

There are six force plates embedded in a circular shape at the center of the sensing structure. The slanted angle of each force plate and ridges on the top surface (Figure. 2-b) facilitates the

planar movement of the force plates. In addition, the protrusion on the side increases the sensitivity of the sidewall to shear forces. The actual prototype with embedded microchannels and force plates is shown in Figure. 2-c.
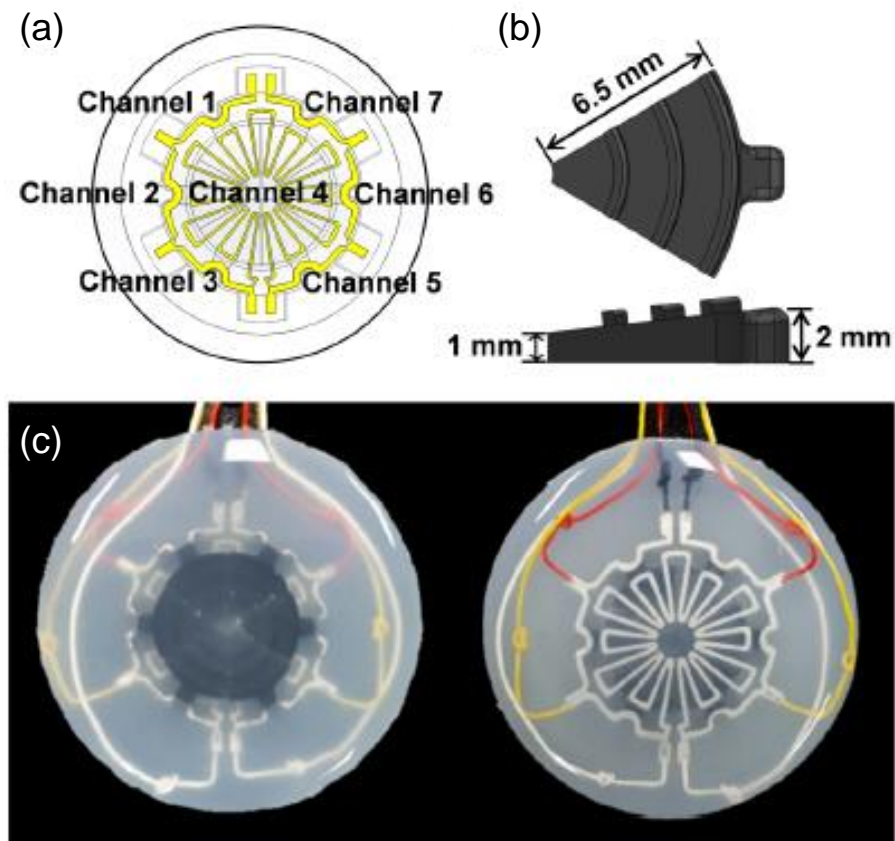


**Figure. 2.** Design of a soft multi-axis load cell (a) Showing embedded microchannels in a soft polymer structure, (b) design of a force-plate, (c) the actual prototype of the sensor.
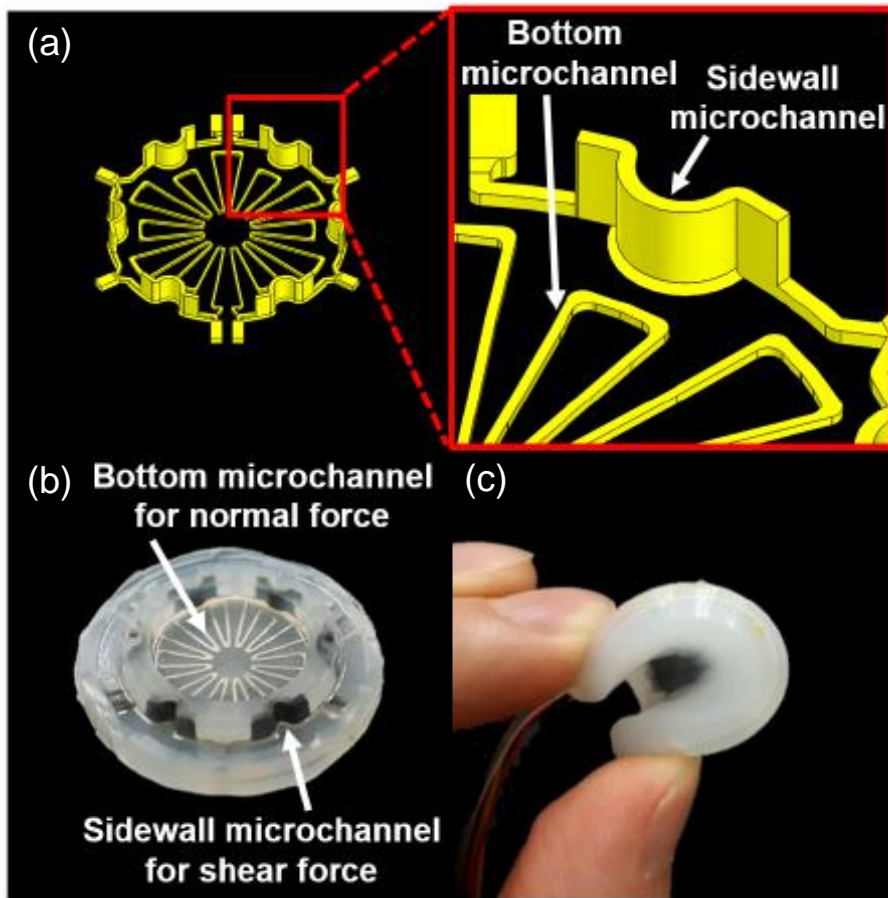
**Figure. 3.** (a) Solid model showing a three−dimensional structure of sidewall microchannels. (b) Internal sensing structure of actual prototype. (c) Deformability of the soft three−axis force sensor.

# Chapter 3. Fabrication

The sensor was fabricated using a layered molding and casting method, as shown in Figure. 4 [15]. First, the internal sensing structure with the microchannels and the force plates is made using a top and a bottom mold. While the top mold has a circular protrusion to make a space for the force plates, the bottom mold has a positive pattern (Figure. 4-a). After being filled with liquid-state silicone (Ecoflex 0030), the bottom mold is covered by the top mold, and any excessive material is squeezed out of the mold. After curing in an oven at 60 ℃ for about 20 minutes, the molds are removed. The next step is to add a flat layer to the bottom of the sensing structure to seal the open microchannels. A thin, flat layer is made by spin-coating, partially cured, bonded to the bottom of the sensing structure (Figure. 4-b), and then fully cured in the oven. After adding signal wires to each microchannel, the housing is formed using stiffer silicone (Dragon Skin 30) with a new mold (Figure. 4-c). The signal wire has a knot for preventing itself from being slipped out although the sensor structure experiences large deformation. A total of six force plates are placed in the empty space of the sensing structure, and soft liquid silicone (Ecoflex 0050) is poured on top to fully enclose the force plates (Figure. 4-d). Before pouring of silicone, a low-friction film is inserted underneath the force plates to help their lateral movements, which

increases the sensitivity to shear forces. Finally, EGaIn is injected into the microchannels using two syringes (Figure. 4-e), and it completes the prototype (Figure. 4-f).
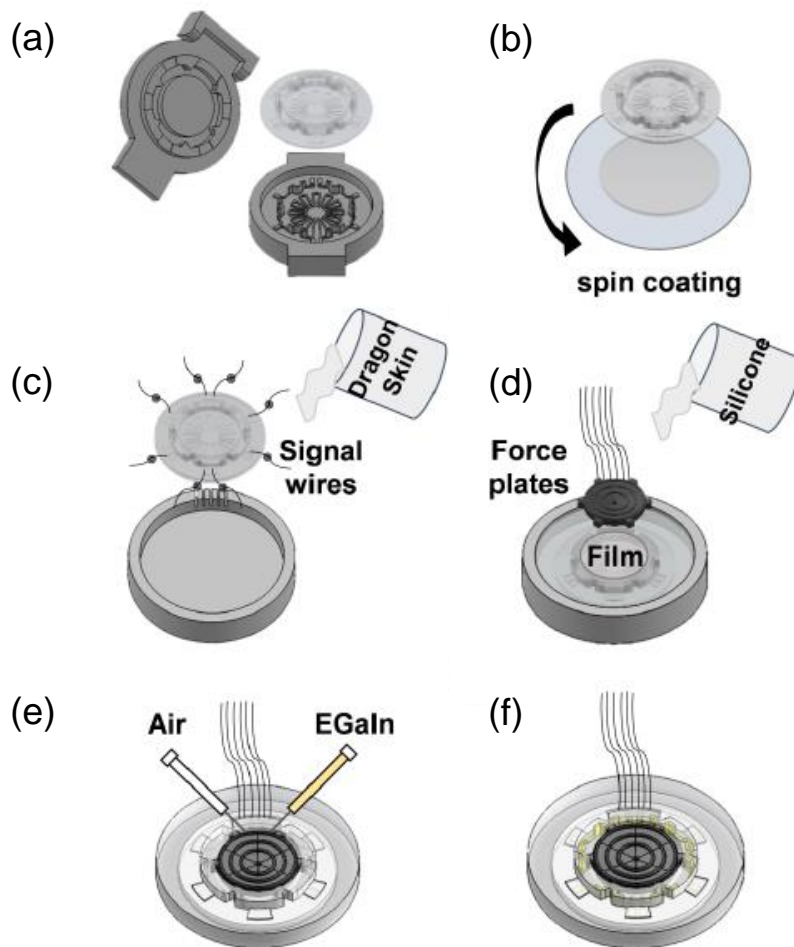
**Figure. 4.** Fabrication process: (a) Molding and casting of 3D microchannel layer, (b) sealing of open-top microchannels using spin-coating, (c) connecting and embedding signal wires, (d) embedding force plates, (e) injecting liquid metal (EGaIn) into microchannels, and (f) complete prototype.

# Chapter 4. Sensor Characterization

## 4.1. Experimental Setup

Our prototype provides a total of seven signal outputs, one from the bottom channel and the other six from the sidewall channels for normal and shear force sensing, respectively. To generate multi-axis forces for experiments, a tabletop computer numerical control (CNC) milling machine (MT-3040B, RM) was modified by installing a hemispherical indenter (diameter: 10 mm) made of rigid plastic (Figure. 5). The CNC machine generates forces in three axes, which are applied to the soft sensor through the indenter. The resistance changes of the corresponding microchannels are then measured by a micro-controller (Arduino Due, SparkFun Electronics) through the custom amplifier circuit. While measuring the soft sensor outputs, the actual force is also measured by a commercial load cell (RFT60-HA01, ROBOTOUS) attached to the bottom of the soft sensor for comparison. The force data is acquired at 40 Hz in both sensors.
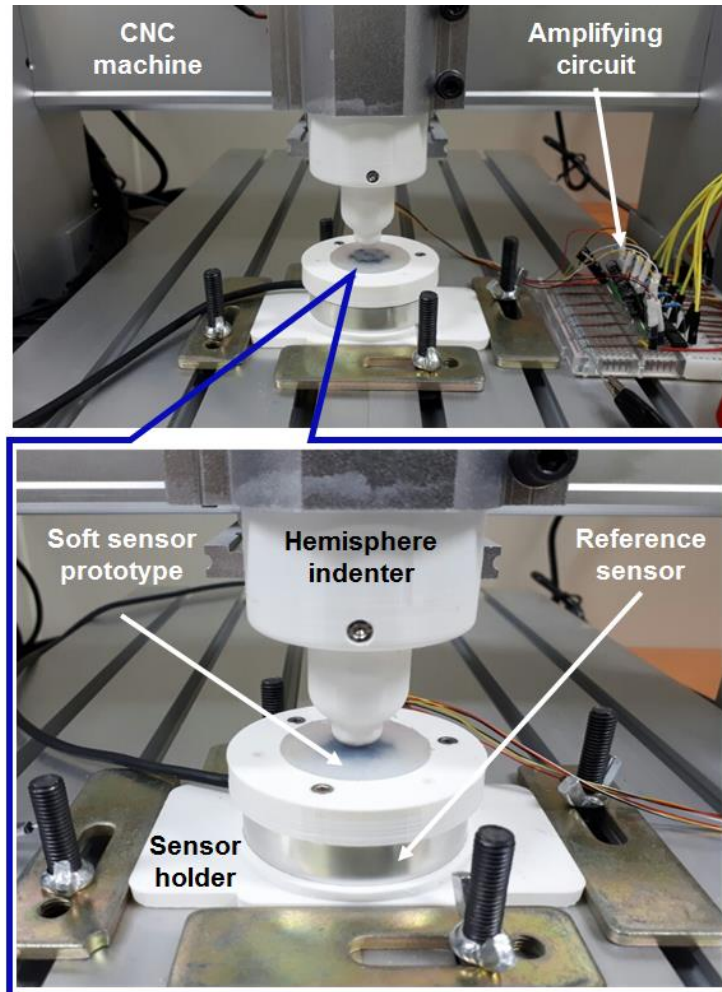
**Figure. 5.** Experimental setup for sensor characterization. CNC machine applies controlled force in three axes through hemispherical indenter, and sensor outputs are collected and compared with those of reference sensor (commercial three-axis load cell).

## 4.1. Characterization result

The soft sensor was experimentally characterized by applying forces in thirteen different directions, one normal direction and twelve planar directions combined with a normal component, as shown in Figure. 6. All the seven microchannels were connected in series, and constant current was applied. During the experiments, the CNC machine applied forces up to 13 N in the planar directions (Fx and Fy) and 35 N in the vertical direction (Fz). The sensor data from both the soft sensor and the commercial load cell are shown in Figure. 6. When a pure z-axis force was applied, only Channel 4 showed a voltage output. When a combined force of x- or y-axis and z-axis was applied, the multiple channels corresponding to the force showed voltage outputs. When a force was applied between two force plates, the two channels corresponding to the force plates showed voltage outputs. Although the sensor had a limited number of the force plates, it was possible to interpolate the sensor signals and to detect forces in more directions than the number of the force plates. When a pure normal force was applied, the output from Channel 4 was high, since the bottom channel was compressed by the entire force plates. However, when a force with a shear component and the same level of a normal component was applied to a specific single force plate, the output from Channel 4 was low because only one force plate compressed the underneath

microchannel. In addition to the force characterization, repeatability was tested, as shown in Figures. 7 to 9. For ten times of normal loading and unloading (Figure. 7) and five times of shear loading and unloading (Figure. 8), the soft sensor generated reliable outputs. Further tests for durability were also conducted. Our soft sensor showed physical robustness and signal reliability for over 1000 cycles of loading and unloading up to 35 N and 7.5 N in normal and shear directions, respectively (Figure. 9).
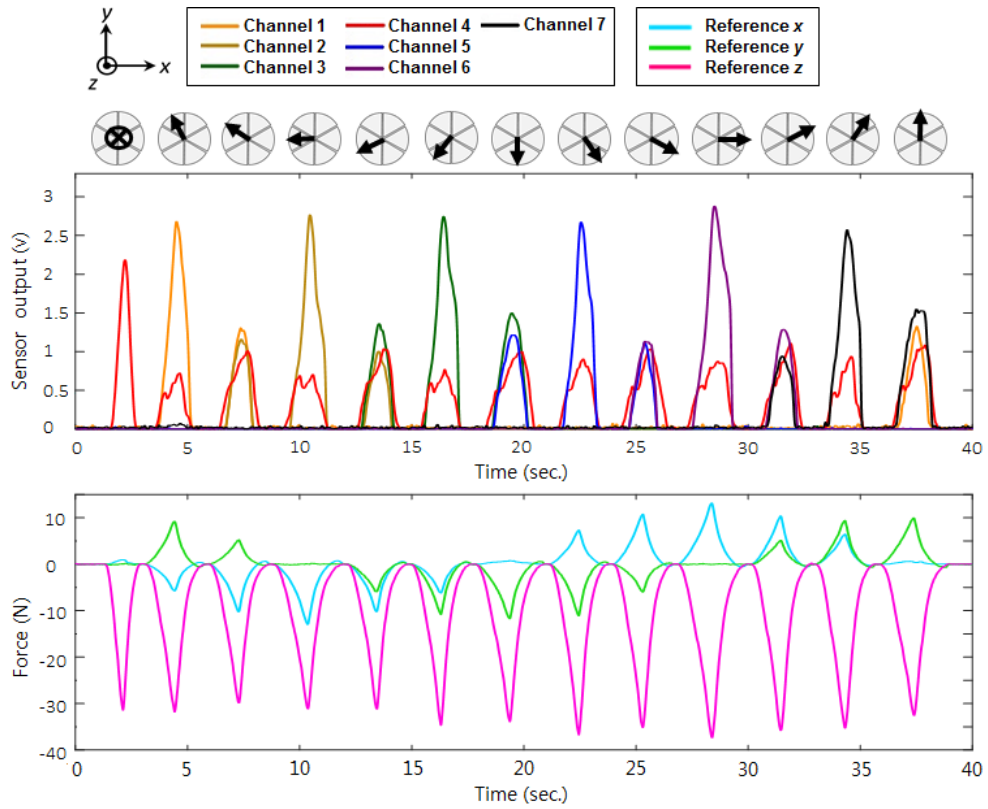
**Figure. 6.** Test result of multi-directional force sensing showing the directions and magnitudes of the applied forces and their corresponding sensor outputs.

**Figure. 7.** The signals from channel 4 by the normal force repeated 10 times
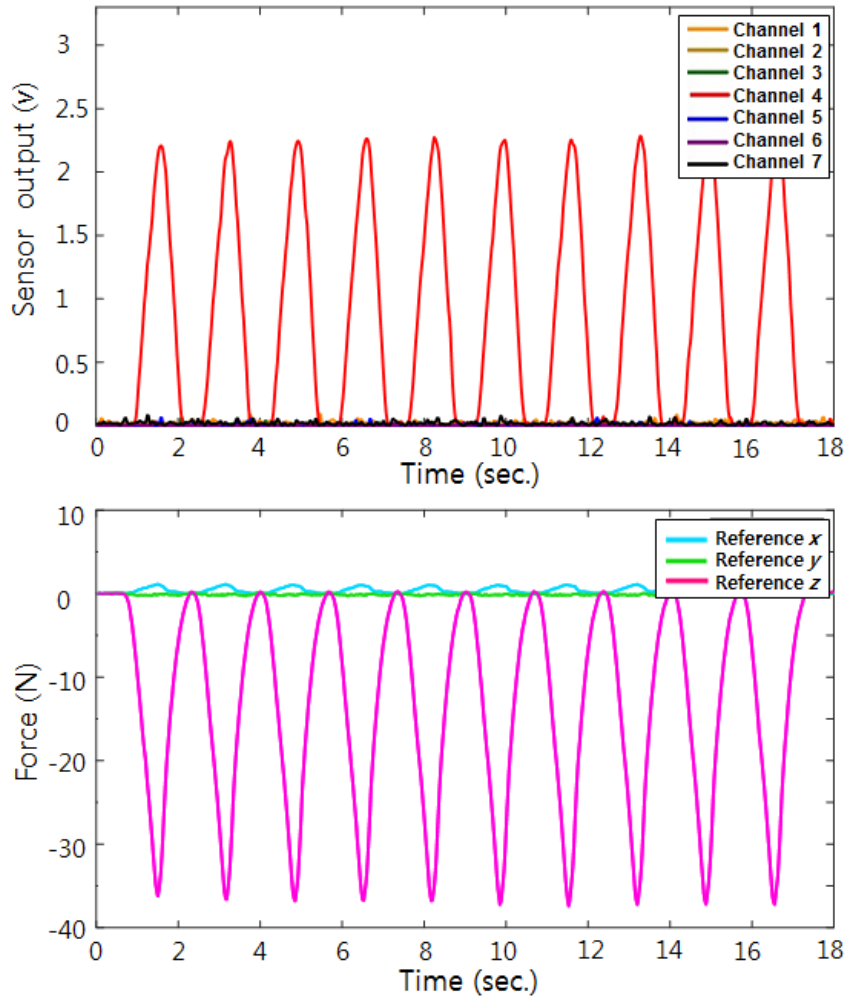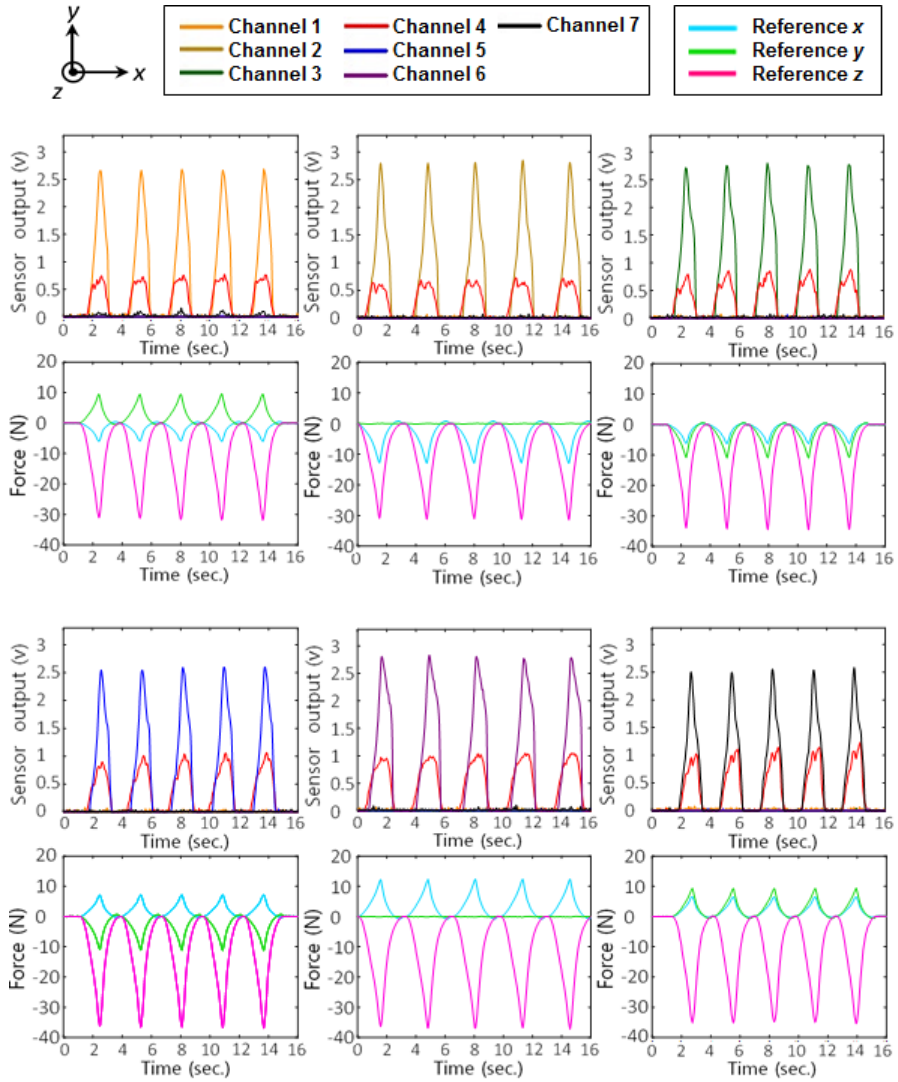
**Figure. 8.** The signals from each sidewall channel by applying forces including both normal and shear force components repeatedly 5 times
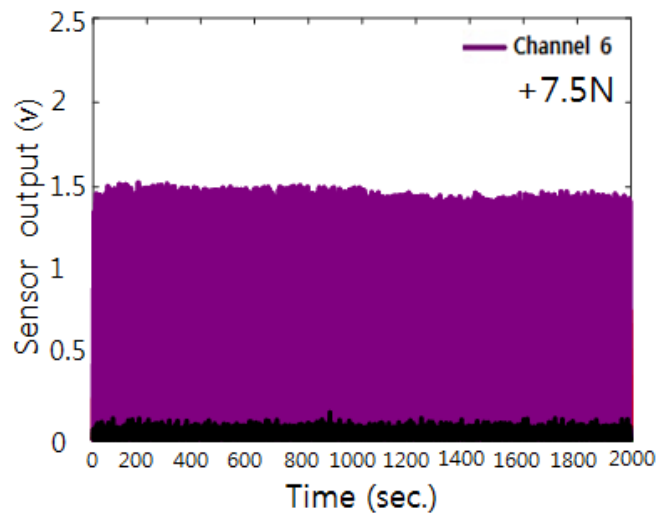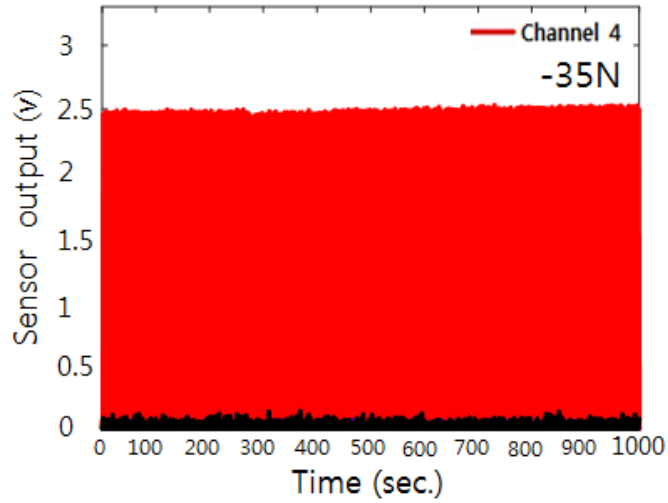
**Figure. 9.** The result of durability test for normal force of $-35$ N during 1000 cycles (top), the result of durability test for shear force sensing with the force of 7.5 N repeated during 1000 cycles (bottom).

# Chapter 5. Materials and Sensor Performance

Since soft sensors made of polymer materials typically show nonlinearity with relatively large hysteresis, which was also observed in our sensor, we fabricated and tested three sensor prototypes with different combinations of silicone elastomers to examine the effect of materials. The main purpose of this test is to find a combination of materials that can alleviate the hysteresis as well as improve the sensitivity in a low force range.

## 5.1. Material Selection

While the elastomer materials for the housing and the microchannel structures were fixed to Dragon Skin 10 and Ecoflex 0030, respectively, three different materials (Ecoflex 0030, Ecoflex 0050, and Dragon Skin 10) were tried for the top structure where

### TABLE I
### MATERIAL PROPERTIES

|  | Shore Hardness (00, A) | 100 % Modulus (ASTM D412) | Elongation at Break |
|---|---|---|---|
| Ecoflex 0030 | 00-30 | 69 kPa | 900 % |
| Ecoflex 0050 | 00-50 | 83 kPa | 980 % |
| Dragon Skin 10 | 10 A | 152 kPa | 1000 % |

the force is applied through the embedded force plates. Table I shows the material properties of the three silicone elastomers.

According to the data sheet and the shore hardness scale provided in [33], Ecoflex 0030 is softer than Ecoflex 0050, and Ecoflex 0050 is softer than Dragon Skin 10.

## 5.2. Experimental Result

The three sensor prototypes were tested by applying two different types of loads, normal force up to 28 N and shear force until the sensor output reached 2.5 V, one by one. The tests were done by making loading and unloading loops for each prototype. The results show that the use of stiffer materials slightly decreased the pressure sensitivity but significantly improved the hysteresis for normal force (Figures. 10-a to 10-c). For shear force, although the stiffer top structure decreased the hysteresis level, it also significantly decreased the sensitivity (Figures. 10-d to 10-f). For example, while -5 N of shear force was required to achieve 2.5 V sensor output for Ecoflex 0030, -16 N of shear force was needed to produce the same level of sensor output for Dragon Skin 10. Therefore, the multi-material structure of our sensor design requires investigations on materials for different applications.
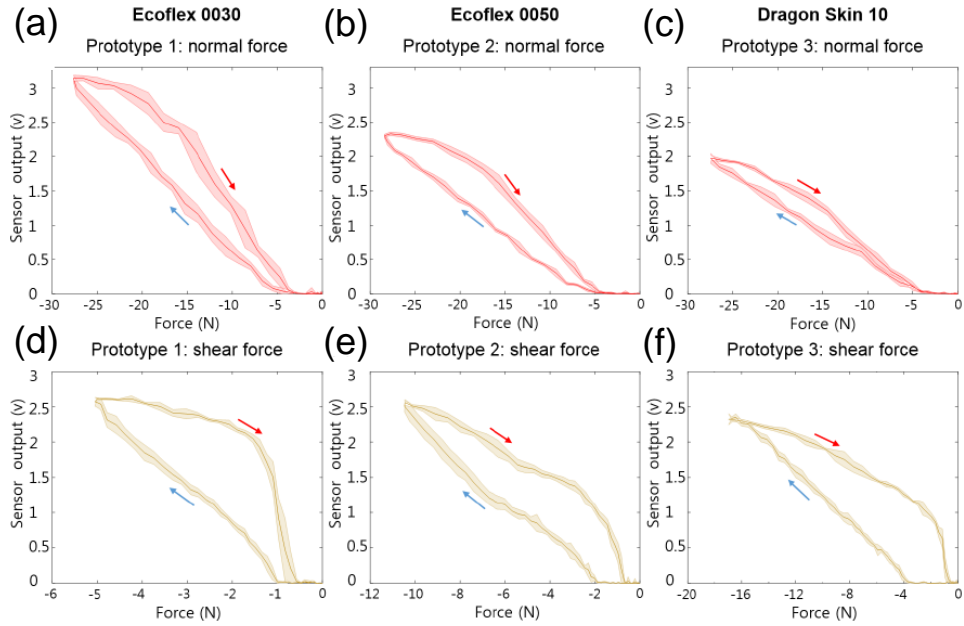
**Figure. 10.** Test result to determine the effect of material combinations on the performance of the soft sensor, (a)－(c) the signals of each prototype for applying only normal forces (d)－(f) the signals for the shear forces applied in the direction corresponding to channel 2, The signal graphs show the hysteresis of each signal and the range of detectable forces depending on the soft sensors composed of different material combination.

# Chapter 6. Calibration using Machine Learning

As shown in Figure. 10, the proposed sensor has two major drawbacks when compared with traditional force sensors: nonlinearity and hysteresis in response, which are easily seen especially in microfluidic soft sensors. These characteristics make it difficult to characterize the system both analytically and experimentally. In addition, since the proposed sensor can generate various combinations of sensing signals based on the magnitude and the direction of the applied forces, the calibration process could be complicated and time-consuming. Therefore, we propose to address these issues by taking advantage of machine learning. We used an artificial neural network (ANN) model, in the calibration state for estimating Fx, Fy and Fz components of contact forces.

## 6.1. Integration with Soft End Effector

To facilitate collection of sensor data for training, we developed a soft end-effector that could be directly integrated with the proposed soft sensor. Figure. 11 shows the design of the end-effector, showing how the soft sensor could be integrated in the middle of the structure. A force post made of a rigid plastic was embedded in the structure instead of force plates for force transmission. The force post has six protrusions on the sides to

increase the sensitivity of the sidewall microchannels for shear force sensing. The top of the end-effector is covered with a spherical silicone cap where physical contacts are made. When a force is applied to the cap, the force post tilts and compresses both the corresponding sidewall and bottom microchannels, making changes in the sensor signal. The extended part of the force post at the bottom is embedded in a silicone structure, which not only limits the range of the tilting angle but also easily restores the original position of the post when the contact is removed.
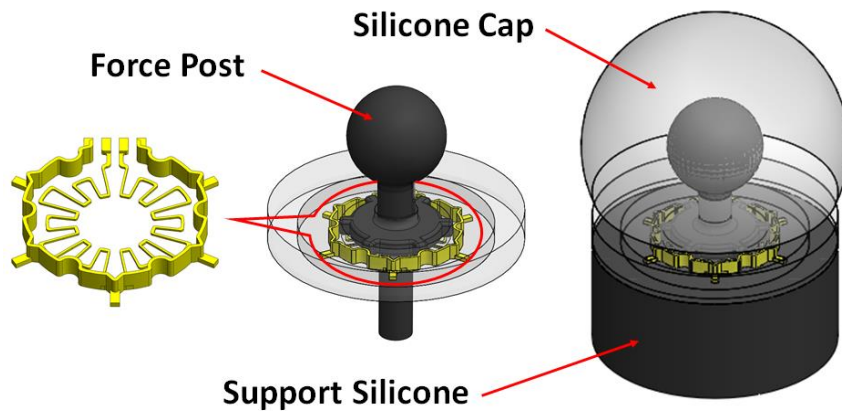


**Figure. 11.** Design of a soft end effector integrated with the proposed soft three-axis load cell.

## 6.2. Learning Method

To obtain training and test data sets, an experimental setup was prepared, as shown in Figure. 12-a. The soft load cell was fixed on a 3D-printed holder and a commercial multi-axis force sensor was installed underneath the holder. Contact force data with varied magnitudes and directions were generated by touching the end-effector multiple times at random. Total of approximately 910 training data sets and 130 test data sets were acquired at a sampling rate of 10 Hz from the proposed sensor and the commercial force sensor. Figures 13-a to 13-d show the training and the test data sets from the soft three-axis load cell and the reference force sensor, respectively.

Artificial neural network with one input (200 units) layer, three hidden (100, 50 and 25 units) layers, and one output layer (3 units) was used to train the system. Since the reference force data sets had negative values, the leaky sigmoid function was set as an activation function and the Adam optimizer was used to minimize the training cost with a base learning rate of 0.001. Training was performed for 1000 epochs, and each update was conducted using 50 sequence lengths. In addition, dropout was also applied to each layer with a 50 % dropout rate to prevent the learning model from overfitting the training data sets.
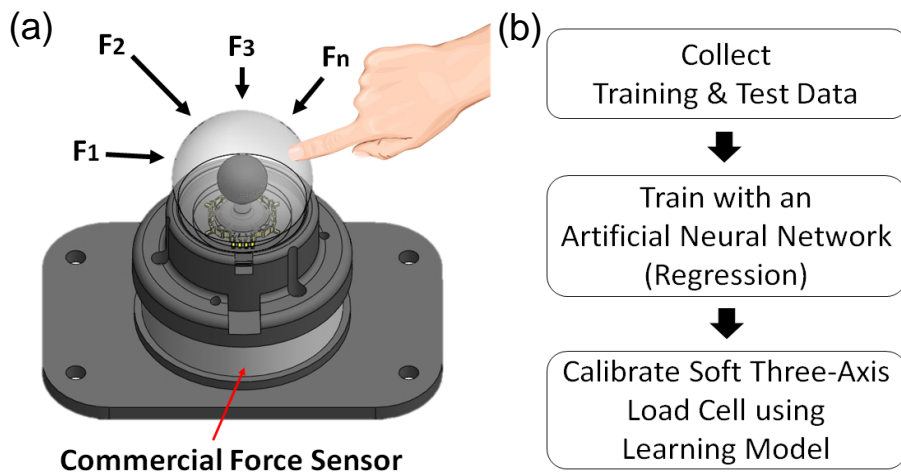
Figure. 12. Calibration process using machine learning. (a) Experimental setup for collecting training and test data with randomly applied external forces to the end-effector with finger touches. (b) Learning process: collection of training and test data (seven output signals from the soft load cell and three force data ($F_x$, $F_y$ and $F_z$) from the commercial force sensor) and training with an artificial neural network (regression using one input, three hidden and one output layers).

**Figure. 13.** Training and test data sets: (a) training data sets from the proposed soft three-axis load cell (analog to digital converted values), (b) training data sets from the reference force sensor (Fx, Fy, and Fz), (c) test data sets from the proposed soft three-axis load cell (analog to digital converted values), and (d) test data sets from the reference force sensor (Fx, Fy, and Fz).
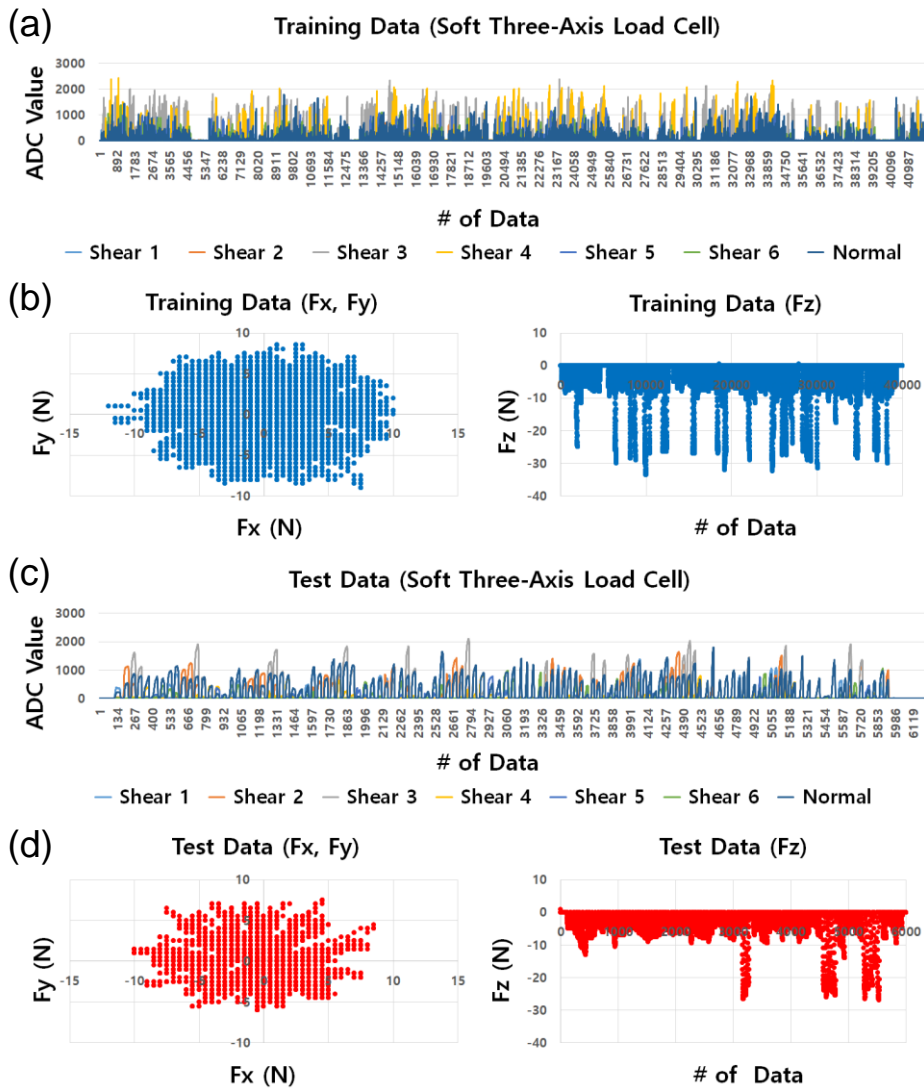
## 6.3. Result

Figure. 14 shows the result force estimation with time using the test data sets. The estimation force values in each axis (x, y and z) match the true values. We used root-mean-square error (RMSE) and normalized RMSE (NRMSE) for a quantitative analysis to evaluate the performance of our learning model as follows:

$$RMSE = \sqrt{\frac{1}{N}\sum_{i=1}^{N}(\hat{y}_i - y_i)^2}$$

$$NRMSE = \frac{RMSE}{y_{\max} - y_{\min}} \times 100\%$$

Table II shows the results of the RMSE and NRMSE corresponding to each force component (Fx, Fy and Fz). The learning model showed NRMSEs of 4.80 %, 5.53 % and 6.42 % for Fx, Fy, and Fz, respectively.

These results demonstrate that the learning model fits sensor data well. Compared with other force estimation results of different soft sensors using neural networks, as shown in Table III, our learning results are in an acceptable range. The normal force and shear force estimation for a footpad sensor [34] showed a NRMSE between 1.17 % and 10.14 % and soft microfluidic pressure sensor [35] had NRMSEs for normal force estimation from 5 % to 8.38 %.
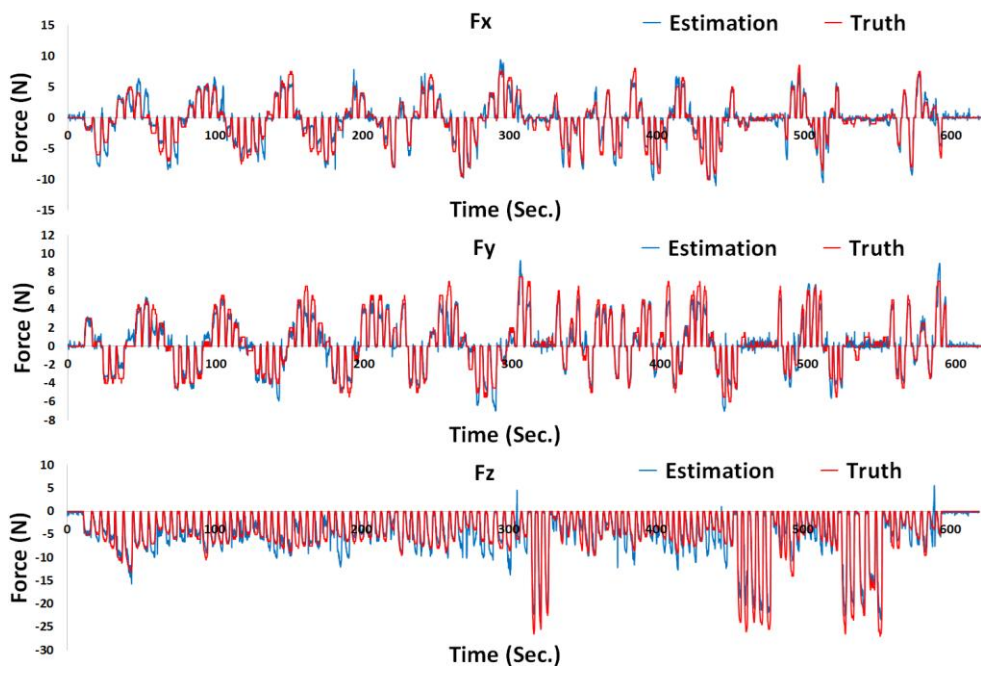
**Figure. 14.** Results of force estimation in three−axis (x, y and z) using test data.

## TABLE II
### LEARNING RESULT OF THREE-AXIS FORCES ESTIMATION

|  | Fx | Fy | Fz |
|---|---|---|---|
| Force Range (N) | $-10-8.5$ | $-6-7.5$ | $-27-0$ |
| RMSE (N) | 0.89 | 0.75 | 1.73 |
| NRMSE (%) | 4.80 | 5.53 | 6.42 |

## TABLE III
### COMPARISON OF MACHINE LEARNING RESULT

|  | NRMSE (%) | | |
|---|---|---|---|
|  | Fx | Fy | Fz |
| Prototype | 4.80 | 5.53 | 6.42 |
| Chuah et al | 1.17 | 10.14 | 8.30 |
| Han et al | - | - | $5-8.38$ |

# Chapter 7. Conclusion

 In this paper, we developed a soft three-axis force sensor with enhanced spatial resolution and improved sensitivity for both normal and shear force sensing. The sensor was made of a combination of silicone elastomers (Ecoflex 0030, Ecoflex 0050, and Dragon Skin 10 from Smooth-On) and embedded microchannels filled with a liquid conductor. When a force is applied to the sensor, the microchannels deform and change the electrical resistance. Based on the direction of the force, only part of the microchannels change the resistance, which is used for detecting the direction of the force. In order to decouple normal and shear force components acting on the sensor, the microchannels were embedded in different locations relative to the force plates. While the bottom microchannel detects normal forces, the sidewall microchannel detects shear forces in multiple directions. In addition, the sidewall channel was divided into six segments with individual output signals for detecting forces in multi-axes. As a result, the proposed sensor was able to measure the applied force in 3D that contains both normal and shear components. Although the experiments tested only twelve directions for shear force sensing, the actual spatial resolution can be much higher if the sensor signals from two force plates are interpolated. Additional experiments were carried out to investigate the effect of the materials. The results showed that the hysteresis

level and the sensitivity could be controlled by changing the combination of the elastomer materials of the sensor. Furthermore, a machine learning technique based on an artificial neural network was employed to calibrate the proposed sensor. The result demonstrated that use of machine learning can make the calibration process easier and more time−efficient.

TABLE IV
COMPARISON OF SOFT THREE-AXIS FORCE SENSORS

|  | Measurment Range | Directly Detectable Force Direction |
|---|---|---|
| Prototype | 0-35 N ($F_z$) 0-13 N ($F_x$, $F_y$) | 1 Normal 12 Tangential |
| Viry et al. [26] | 0-13 N ($F_z$) 0-1.8 N ($F_x$, $F_y$) | 1 Normal 8 Tangential |
| Vogt et al. [28] | 0-5 N ($F_z$) 0-1 N ($F_x$, $F_y$) | 1 Normal 6 Tangential |
| Shi et al. [29] | 0-10 N ($F_z$) 0-40 N ($F_x$, $F_y$) | 1 Normal 4 Tangential |

Although there have been soft sensors that can detect multi−axis force using either piezoresistive materials or liquid conductors [26], [28], [29], the main contribution of this work is to propose a new design of the sensor structure that can mechanically decouple shear force components from a normal force, which increases the sensitivity in shear directions. To achieve this, we developed a fabrication method for a three−dimensional microchannel structure embedded in the soft sensor structure. Furthermore, the idea of

multi−segmented force plates not only decreased the thickness of the sensor but also increased the spatial resolution of shear force sensing. Table IV compares our sensor with a previously developed soft multi−axis sensor.

Although the current work demonstrated force sensing capability in three dimensions with a soft structure, there is still room for improvement. Our immediate future work will be the implementation and testing of our sensors to soft robots for high physical interactions with humans [36], [37], [38]. The mechanical compliance of the sensor not only will increase the compatibility of robots or machines but also can easily conform to complex curved surfaces making itself highly useful to be implemented in various types of existing devices, as discussed in [39]. Another future work will be developing an easier, automatic fabrication method using rapid prototyping equipment to increase repeatability of sensor performance.

# Bibliography

[1] J. Burgner-Kahrs, D. C. Rucker, and H. Choset, "Continuum robots for medical applications: A survey," IEEE Trans. Rob., vol. 31, no. 6, pp. 1261-1280, 2015.

[2] T. Ranzani, G. Gerboni, M. Cianchetti, and A. Menciassi, "A bioinspired soft manipulator for minimally invasive surgery," Bioinspiration Biomimetics, vol. 10, no. 3, p. 035008, 2015.

[3] Y.-L. Park, B.-R. Chen, N. O. P´erez-Arancibia, D. Young, L. Stirling, R. J. Wood, E. C. Goldfield, and R. Nagpal, "Design and control of a bio-inspired soft wearable robotic device for ankle-foot rehabilitation," Bioinspiration Biomimetics, vol. 9, no. 1, p. 016007, 2014.

[4] Y. Ding, I. Galiana, A. T. Asbeck, S. M. M. De Rossi, J. Bae, T. R. T. Santos, V. L. de Araujo, S. Lee, K. G. Holt, and C. Walsh, "Biomechanical and physiological evaluation of multi-joint assistance with soft exosuits," IEEE Trans. Neural Syst. Rehabil. Eng., vol. 25, no. 2, pp. 119-130, 2017.

[5] T. Takayama, H. Takeshima, T. Hori, and T. Omata, "A twisted bundled tube locomotive device proposed for in-pipe mobile

robot," IEEE/ASME Trans. Mechatron., vol. 20, no. 6, pp. 2915–2923, 2015. [6] M. T. Tolley, R. F. Shepherd, B. Mosadegh, K. C. Galloway, M. Wehner, M. Karpelson, R. J. Wood, and G. M. Whitesides, "A resilient, untethered soft robot," Soft Rob., vol. 1, no. 3, pp. 213–223, 2014.

[7] S. Gong,W. Schwalb, Y.Wang, Y. Chen, Y. Tang, J. Si, B. Shirinzadeh, and W. Cheng, "A wearable and highly sensitive pressure sensor with ultrathin gold nanowires," Nat. Commun., vol. 5, p. 3132, 2014.

[8] S. Lee, S. Shin, S. Lee, J. Seo, J. Lee, S. Son, H. J. Cho, H. Algadi, S. Al–Sayari, D. E. Kim et al., "Ag nanowire reinforced highly stretchable conductive fibers for wearable electronics," Adv. Funct. Mater., vol. 25, no. 21, pp. 3114–3121, 2015.

[9] S. Yao and Y. Zhu, "Wearable multifunctional sensors using printed stretchable conductors made of silver nanowires," Nanoscale, vol. 6, no. 4, pp. 2345–2352, 2014.

[10] E. Roh, B.–U. Hwang, D. Kim, B.–Y. Kim, and N.–E. Lee, "Stretchable, transparent, ultrasensitive, and patchable strain sensor for human–machine interfaces comprising a nanohybrid of carbon nanotubes and conductive elastomers," ACS nano, vol. 9,

no. 6, pp. 6252–6261, 2015.

[11] J. T. Muth, D. M. Vogt, R. L. Truby, Y. Meng¨uc ̧, D. B. Kolesky, R. J. Wood, and J. A. Lewis, "Embedded 3d printing of strain sensors within highly stretchable elastomers," Adv. Mater., vol. 26, no. 36, pp. 6307–6312, 2014.

[12] S. Araby, Q. Meng, L. Zhang, H. Kang, P. Majewski, Y. Tang, and J. Ma, "Electrically and thermally conductive elastomer/graphene nanocomposites by solution mixing," Polymer, vol. 55, no. 1, pp. 201– 210, 2014.

[13] C. S. Boland, U. Khan, G. Ryan, S. Barwich, R. Charifou, A. Harvey, C. Backes, Z. Li, M. S. Ferreira, M. E. M¨obius et al., "Sensitive electromechanical sensors using viscoelastic graphene polymer nanocomposites," Science, vol. 354, no. 6317, pp. 1257– 1260, 2016.

[14] C. S. Boland, U. Khan, C. Backes, A. O' Neill, J. McCauley, S. Duane, R. Shanker, Y. Liu, I. Jurewicz, A. B. Dalton et al., "Sensitive, highstrain, high–rate bodily motion sensors based on graphene–rubber composites," ACS nano, vol. 8, no. 9, pp. 8819– 8830, 2014.

[15] Y.-L. Park, B.-R. Chen, and R. J.Wood, "Design and fabrication of soft artificial skin using embedded microchannels and liquid conductors," IEEE Sens. J., vol. 12, no. 8, pp. 2711-2718, 2012.

[16] B. Li, Y. Gao, A. Fontecchio, and Y. Visell, "Soft capacitive tactile sensing arrays fabricated via direct filament casting," Smart Mater. Struct., vol. 25, no. 7, p. 075009, 2016.

[17] A. Frutiger, J. T. Muth, D. M. Vogt, Y. Meng˙˙uc¸, A. Campo, A. D. Valentine, C. J. Walsh, and J. A. Lewis, "Capacitive soft strain sensors via multicore-shell fiber printing," Adv. Mater., vol. 27, no. 15, pp. 2440-2446, 2015.

[18] M. Hu, X. Cai, Q. Guo, B. Bian, T. Zhang, and J. Yang, "Direct pen writing of adhesive particle-free ultrahigh silver salt-loaded composite ink for stretchable circuits," ACS nano, vol. 10, no. 1, pp. 396-404, 2015.

[19] J.-B. Chossat, Y.-L. Park, R. J. Wood, and V. Duchaine, "A soft strain sensor based on ionic and metal liquids," IEEE Sens. J., vol. 13, no. 9, pp. 3405-3414, 2013.

[20] J.-Y. Sun, C. Keplinger, G. M. Whitesides, and Z. Suo, "Ionic

skin," Adv. Mater., vol. 26, no. 45, pp. 7608–7614, 2014.

[21] J.-B. Chossat, H.-S. Shin, Y.-L. Park, and V. Duchaine, "Soft tactile skin using an embedded ionic liquid and tomographic imaging," J. Mech. Rob., vol. 7, no. 2, p. 021008, 2015.

[22] C. Larson, B. Peele, S. Li, S. Robinson, M. Totaro, L. Beccai, B. Mazzolai, and R. Shepherd, "Highly stretchable electroluminescent skin for optical signaling and tactile sensing," Science, vol. 351, no. 6277, pp. 1071–1074, 2016.

[23] J. Guo, X. Liu, N. Jiang, A. K. Yetisen, H. Yuk, C. Yang, A. Khademhosseini, X. Zhao, and S.-H. Yun, "Highly stretchable, strain sensing hydrogel optical fibers," Adv. Mater., vol. 28, no. 46, pp. 10 244–10 249, 2016.

[24] G. Cai, J. Wang, K. Qian, J. Chen, S. Li, and P. S. Lee, "Extremely stretchable strain sensors based on conductive self-healing dynamic cross-links hydrogels for human-motion detection," Adv. Sci., vol. 4, no. 2, 2017.

[25] H. Zhao, K. O' Brien, S. Li, and R. F. Shepherd, "Optoelectronically innervated soft prosthetic hand via stretchable optical waveguides," Sci. Robot., vol. 1, no. 1, p. eaai7529, 2016.

[26] L. Viry, A. Levi, M. Totaro, A. Mondini, V. Mattoli, B. Mazzolai, and L. Beccai, "Flexible three-axial force sensor for soft and highly sensitive artificial touch," Adv. Mater., vol. 26, no. 17, pp. 2659-2664, 2014.

[27] P. Roberts, D. D. Damian, W. Shan, T. Lu, and C. Majidi, "Soft matter capacitive sensor for measuring shear and pressure deformation," in Proc. IEEE Int. Conf. Rob. Autom., Karlsruhe, Germany, May 2013, pp. 3529-3534.

[28] D. M. Vogt, Y.-L. Park, and R. J. Wood, "Design and characterization of a soft multi-axis force sensor using embedded microfluidic channels," IEEE Sens. J., vol. 13, no. 10, pp. 4056-4064, 2013.

[29] X. Shi, C.-H. Cheng, Y. Zheng, and P. Wai, "An egain-based flexible piezoresistive shear and normal force sensor with hysteresis analysis in normal force direction," J. Micromech. Microeng., vol. 26, no. 10, p. 105020, 2016.

[30] T. Kim and Y.-L. Park, "Design of a soft 3-axis load cell for humanrobot interactions," in Proc. Int. Conf. Ubiquitous Rob. Ambient Intell., Jeju, Korea, June 2016, pp. 956-957.

[31] T. Kim, Y.-L. Park, "A soft 3-axis load cell using liquid-filled 3-D microchannels in a highly deformable elastomer", *IEEE Robot. Autom. Lett.*, vol. 3, no. 2, pp. 881-887, Apr 2018.

[32] Y.-L. Park, C. Majidi, R. Kramer, P. B´erard, and R. J. Wood, "Hyperelastic pressure sensing with a liquid-embedded elastomer," J. Micromech. Microeng., vol. 20, no. 12, p. 125029, 2010.

[33] J. L. Alves, A. Silva, T. Duarte, S. Olhero, and J. Ferreira, "Design silicone moulds for manufacturing ceramic microcomponents," Revista da Associac¸˜ao Portuguesa de An´alise Experimental de Tens˜oes, vol. 22, pp. 93–98, 2013.

[34] M. Y. Chuah and S. Kim, "Improved normal and shear tactile force sensor performance via least squares artificial neural network (lsann)," in Proc. 2016 IEEE Int. Conf. Robot. Autom., May 2016, pp. 116–122.

[35] S. Han, T. Kim, D. Kim, Y.-L. Park, and S. Jo, "Use of deep learning for characterization of microfluidic soft sensors," IEEE Robotics and Automation Letters, vol. 3, no. 2, pp. 873–880, 2018.

[36] P. Ohta, L. Valle, J. King, K. Low, J. Yi, C. G. Atkeson, and Y.-L. Park, "Design of a lightweight, soft robotic arm using pneumatic artificial muscles and inflatable sleeves," Soft Rob., 2017.

[37] J. D. Greer, T. K. Morimoto, A. M. Okamura, and E. W. Hawkes, "Series pneumatic artificial muscles (sPAM) and application to a soft continuum robot," in Proc. IEEE Int. Conf. Rob. Autom., Singapore, May 2017, pp. 5503–5510.

[38] R. Qi, A. Khajepour, W. W. Melek, T. L. Lam, and Y. Xu, "Design, kenematics, and control of a multijoint soft inflatable arm for humansafe interaction," IEEE Trans. Rob., vol. 33, no. 3, pp. 594–609, 2017.

[39] C. Majidi, "Soft robotics: A perspective-current trends and prospects for the future," Soft Rob., vol. 1, no. 1, pp. 5–11, 2013.

# Abstract

  소프트 로봇 기술이 발전함에 따라 인간과 로봇 간에 물리적 상호 작용이 발생하는 다양한 어플리케이션에서 소프트 센서의 필요성이 증대되었다. 따라서 본 논문에서는 여러 가지 종류의 탄성중합체로 이루어진 실리콘 구조 내부에 압축력에 민감하게 반응하는 액체금속이 채워진 마이크로채널과 6조각으로 나누어진 힘을 전달하는 힘 플레이트가 내장된 형태의 소프트 다축 힘 센서를 제안한다. 마이크로채널은 3축의 힘을 감지하기 위해 기하학적으로 여러 구획으로 나누어져 있는데 센서의 중앙 아래에는 힘의 수직성분을 측정하는 바닥 마이크로채널이 위치하고 센서의 측면에는 입체적인 구조로 측면 3D 마이크로채널이 위치하고 있다. 센서의 측정 원리는 상부 중앙 표면에 힘이 가해지게 되면 가해진 힘의 방향에 해당하는 힘 플레이트가 이동하면서 바닥과 측면에 마이크로채널을 압축시켜 채널 단면적에 변화를 일으킨다. 이 때 바닥과 측면 채널의 저항변화를 각각 읽어 들임으로써 수직력과 전단력을 기계적으로 완전히 분리하여 측정하는 것이 가능하게 된다. 본 논문에서는 제안하는 센서의 디자인과 제작 방법을 기술하고 센서 특성화를 위해 실험한 데이터를 분석한다. 그리고 제안하는 센서가 내장된 형태의 소프트 엔드 이팩터를 제작하여 데이터를 수집하고 머신러닝 기법을 활용해 데이터를 학습하여 센서의 캘리브레이션 효과적으로 수행하는 방법을 소개한다.